Environmental Science and Ecotechnology 22 (2024) 100471

Contents lists available at ScienceDirect

Environmental Science and Ecotechnology

journal homepage: www.journals.elsevier.com/environmental-science-and-ecotechnology/

Original Research

Polystyrene microplastics and di-2-ethylhexyl phthalate co-exposure: Implications for female reproductive health

Ke Xu, Yunyi Wang, Xiao Gao, Zhaolan Wei, Qi Han, Shuxin Wang, Wanting Du, Jian Wan, Cuihong Wan, Mingqing Chen *

School of Life Sciences, Central China Normal University, Wuhan, 430079, Hubei, China

ARTICLE INFO

Article history:
Received 5 March 2024
Received in revised form
26 July 2024
Accepted 29 July 2024

Keywords:
Microplastics
DEHP
Reproductive toxicity
PCOS
TGF-β1/Smad3

ABSTRACT

Microplastics and phthalates are prevalent and emerging pollutants that pose a potential impact on human health. Previous studies suggest that both microplastics and phthalates can adversely affect the reproductive systems of humans and mammals. However, the combined impact of these pollutants on the female reproductive system remains unclear. Here we show the impacts of exposure to polystyrene microplastics (PS-MPs) and di-2-ethylhexyl phthalate (DEHP) on female Sprague-Dawley rats' reproductive systems. We find that co-exposure to PS-MPs and DEHP results in a marked increase in cystic and atretic follicles, oxidative stress, fibrosis, and dysregulation of serum sex hormone homeostasis in the ovaries of the rats. Proteomic analysis identified differentially expressed proteins that were predominantly enriched in signaling pathways related to fatty acid metabolism and tight junctions, regulated by transforming growth factor β1 (TGF-β1). We further confirm that co-exposure to DEHP and PS-MPs activates the TGF-β1/Smad3 signaling pathway, and inhibiting this pathway alleviates oxidative stress, hormonal dysregulation, and ovarian fibrosis. These results indicate that exposure to the combination of microplastics and phthalates leads to a significant increase in atretic follicles and may increase the risk of polycystic ovary syndrome (PCOS). Our study provides new insights into the reproductive toxicity effects of microplastics and DEHP exposure on female mammals, highlighting the potential link between environmental pollutants and the occurrence of PCOS. These findings highlight the need for comprehensive assessments of the reproductive health risks posed by microplastic pollution to women and contribute to the scientific basis for evaluating such risks.

1. Introduction

Microplastic pollution is considered one of the most pressing issues in the fields of ecological and environmental sciences [1]. The annual production of nonbio-based or nonbiodegradable plastic products exceeded 390 million metric tons in 2021, with the demand increasing [2]. Despite the increased attention paid to plastic recycling, plastic products usually end up in landfill sites (about 23%) or the wild. Depending on particle diameter, plastic particles are defined as microplastics (MPs, <5 mm) and nanoplastics (NPs, <100 nm) [3]. Plastic particles are universally found in water, food, and air [4,5]. Evidence shows that MPs (0.2–0.5 μm) can unintentionally move along the food chain [6], but they are also intentionally added to everyday products, such as cosmetics and abrasive cleaners [7]. Data suggest that humans can ingest up to 5 g MPs per week via multiple routes of exposure [8]. Given the ubiquity of MPs in the environment, people inevitably inhale or ingest them daily. Therefore, evaluating the risks of exposure to MPs is an urgent public health priority.

MPs do not exist in isolation in the environment, as plasticizers often coexist with MPs, from marine products to animal feed [9,10]. On the one hand, plasticizers make up a large proportion of polymer additives and can account for up to 40–70% (w/w) of a plastic product [11,12]. MPs will also contain plasticizers, which can be released when plastic products degrade. On the other hand, MPs also have relatively large surface areas, enabling them to pick up other environmental pollutants, including di-2-ethylhexyl phthalate (DEHP) and heavy metal ions. DEHP is a commonly used

* Corresponding author. School of Life Sciences, Central China Normal University, Building 5, No.152 Luo-Yu Road, Wuhan, 430079, China.
E-mail address: chenmq@mail.ccnu.edu.cn (M. Chen).

https://doi.org/10.1016/j.ese.2024.100471

plasticizer that can adsorb more on the surface of MPs than several other common plasticizers [13]. Humans can be exposed to both MPs and DEHP via oral ingestion, inhalation, and dermal contact, putting them at risk of being exposed to both MPs and DEHP simultaneously. However, most current studies focus on a single component of MPs and neglect the effects of plasticizers commonly found adsorbed to MPs.

Studies of exposure to either MPs or DEHP are increasing, but research into exposure to a combination of the two is relatively rare. Wang et al. demonstrated that MPs (5 μm) may cross the blood-brain barrier, thereby impairing the cognitive abilities of mice in terms of learning and memory [14]. Furthermore, one of our previous studies proved that polystyrene microplastics (PS-MPs) could damage the blood-testis barrier, resulting in reproductive system injury through oxidative stress and activation of the p38 MAPK signaling pathway in male mice [15]. Other studies have reported that PS-MPs can collect in the testes of mice, impairing sperm quality and reducing testosterone levels [16,17]. Organisms that ingest MPs contaminated with toxic chemicals may be exposed to high health risks, as these chemicals may be carried into tissues by the host plastic particles [18]. Recent studies have indicated that phthalates adsorbed to MPs increase intestinal damage [13] and cause dysgenesis [19] in male mice. A small number of female-mice-based studies suggest that exposure to PS-MPs induces ovarian inflammation, reduces oocyte quality, and results in ovarian granule apoptosis and reduction in growing follicles [2,20]; it also appears that the female reproductive system is more sensitive to the adverse effects of MPs than the male reproductive system is [21]. Oxidative stress is one of the main pathways by which MPs induce reproductive toxicity. The ovary is also one of the target organs of DEHP. Human epidemiological studies have found a relationship between DEHP exposure and adverse reproductive health outcomes in both men and women [22,23]. However, the impacts and mechanisms of exposure to a combination of MPs and phthalates on the female reproductive system remain unexplored.

In the context of declining fertility rates worldwide, pollution may be one of the underlying causes. The combined pollution from MPs and plasticizers may present a significant challenge to female fertility. Polycystic ovary syndrome (PCOS) is a familiar female reproductive illness characterized by hyperandrogenism, polycystic ovarian morphology [24,25], and ovarian fibrosis, affecting 6–20% of women of childbearing age [26]. Until now, the pathogenesis of PCOS has been unclear. Oxidative stress and TGF-β1/Smad3 signaling transduction are widely observed in PCOS [27,28]. Ovarian damage caused by oxidative stress can introduce fibrosis in the ovaries, resulting in decreased ovarian function. It has been proven that TGF-β1/Smad3 plays a vital role in fibrotic disease in tissues [29,30] and in the conversion of estrogens and androgens [31].

This research explored whether co-exposure to DEHP and PS-MPs leads to PCOS-like features in rat ovaries, such as increased cystic follicles, dysregulation of sex hormone homeostasis, oxidative stress, and fibrosis. We also explored the specific mechanisms of ovarian damage caused by single or combined exposure to MPs and DEHP in Sprague-Dawley (SD) rats.

2. Materials and methods

2.1. Chemicals and kits

PS-MPs (0.2–0.5 μm) were purchased from Macklin Biochemical Corporation. The size was determined using a scanning electron microscope (SEM, JSM-6700F, JEOL), and the chemical composition was characterized using Raman spectroscopy (HORIBA Jobin Yvon). Fig. S1 (Supplementary Material) shows photographs of the PS-MPs. DEHP was obtained from Sigma-Aldrich (D201154). The PS-MPs and DEHP solutions were ultrasonically mixed for half an hour before use to ensure uniform mixing.

2′,7-dichlorodihydrofluorescein (DCFH-DA, St. Louis, Missouri) was used to determine reactive oxygen species (ROS) levels. Superoxide dismutase (SOD) activity was examined using a SOD assay kit (Nanjing Jiancheng, China). A bicinchoninic acid (BCA) kit (Vazyme Biotech Co., Ltd. Nanjing, China) was used to measure protein concentration. All enzyme-linked immune sorbent assay (ELISA) kits, including TGF-β1, estradiol (E2), testosterone (T), collagen I (COL1A1), and collagen III (COL3A1), were obtained from Shanghai Enzyme-linked Biotechnology Co., Ltd (Shanghai, China). The quantitative real-time polymerase chain reaction (qRT-PCR) related reagents were manufactured by Accurate Biology (Hunan, China).

2.2. Animals

Forty-eight five-week-old (160–180 g) healthy female SD rats were obtained from the China Three Gorges University. The animals were acclimated to feeding for a week while housed in a specific pathogen free laboratory animal center at a temperature of 25 ± 3 °C, humidity of 50–70%, and a light–dark cycle of 12 h. Food and water were provided ad libitum. All treatments followed the guidelines in "Animals Research: Reporting In Vivo Experiments" [32] with ethics board approval (CCNU-IACUC-2022-005).

2.3. Experiment design

Thirty of the SD rats were randomly assigned to five groups ($n = 6$): (1) the saline group, (2) the MP group (PS-MPs: 5 mg per kg^{-1} d^{-1}), (3) the DEHP group (DEHP: 3 mg kg^{-1} d^{-1}), (4) the MP + L-DEHP group (PS-MPs: 5 mg kg^{-1} d^{-1}; DEHP: 0.3 mg kg^{-1} d^{-1}), and (5) the MP + H-DEHP group (PS-MPs: 5 mg kg^{-1} d^{-1}; DEHP: 3 mg kg^{-1} d^{-1}). The PS-MPs dose was chosen based on environmental human exposure levels, as reported in previous studies [8], and on the body–surface area ratio. The DEHP exposure doses (0.3, 3 mg kg^{-1} d^{-1}) were calculated based on the tolerable daily intake (48 μg per kg bw per d) [34] and the body–surface area ratio. To confirm the role of the TGF-β1/Smad3 pathway, SIS3, a selective inhibitor of Smad3, was administered by intraperitoneal injection, with a dose chosen based on the experiments conducted by Wu et al. [33]. The remaining 18 rats were randomly assigned to the following three groups ($n = 6$): (6) the SIS3 group (SIS3: 1.25 mg kg^{-1} 3 d^{-1}), (7) the MP + SIS3 group (PS-MPs: 5 mg kg^{-1} d^{-1}; SIS3: 1.25 mg kg^{-1} 3 d^{-1}), and (8) the MP + H-DEHP + SIS3 group (PS-MPs: 5 mg kg^{-1} d^{-1}; DEHP: 3 mg kg^{-1} d^{-1}; SIS3: 1.25 mg kg^{-1} 3 d^{-1}).

The suspensions were administered by intragastric gavage daily for 42 days. The rats were weighed between 9 a.m. and 10 a.m. each day. All animals were euthanized within 24 h following the last gavage, and the tissues and blood were collected for later analysis. The specific experimental protocol is shown in Fig. S2 (Supplementary Material). The ovaries from each group were homogenized individually with phosphate-buffered saline. All samples were centrifuged at 12,000 rpm at 4 °C for 15 min. The supernatant was stored at −80 °C for later assessment.

2.4. Hematoxylin-eosin staining and follicle count

The ovarian tissues were fixed, dehydrated, and embedded in paraffin. These were then sliced and stained with hematoxylin-eosin (H&E), as described in our previous study [35]. All sections were photographed with an Olympus BX73 microscope. According to previous studies, rat follicles were classified into one of five categories: primordial follicles, primary follicles, secondary

follicles, cystic follicles, and corpus luteum [36,37]. Atretic follicles are defined as follicles that stop growing and progressively degenerate during development in the ovary. Two investigators categorized and counted follicles in all fields of view (under 20 × magnification) based on the above follicle classifications.

2.5. Masson's trichrome staining

The four-μm-thick sections of ovarian tissue were stained with Masson's trichrome, according to the procedure described in a previous study [38], to evaluate the degree of collagen deposition in the ovaries. Images were obtained using a Nano Zoomer S360 slide scanner (Hamamatsu, Japan). The area of the blue stain was estimated using Image J software, and the area of fibrosis was expressed as a proportion of the total area of the ovary. For each section, five observation fields were randomly selected.

2.6. ELISA

The concentrations of E2 (pmol mL^{-1}) and T (pg mL^{-1}) in serum and the TGF-β1 (ng mL^{-1}), COL1A1 (μg L^{-1}), and COL3A1 (μg L^{-1}) levels in ovarian homogenate supernatant were quantified using ELISA kits. According to the manufacturer's protocols, the samples were mixed with the kit reagents, washed five times, added to the chromogenic solution for 20 min, and finally treated with the stop solution. The absorbance of each specimen was read using a microplate reader (Bio-Tek Synergy-2, USA) at 450 nm. The concentrations were computed according to the normal curve diagram.

2.7. Assessment of oxidative stress markers in ovarian tissue

The supernatant of the ovarian homogenate was used to detect oxidative stress markers. Briefly, 100 μL supernatant was mixed with 100 mM DCFH-DA for half an hour at 37 °C to determine ROS levels. The degree of light emitted was read using a microplate reader at 485/525 nm wavelength. Malondialdehyde (MDA) was quantitatively determined using a thiobarbituric acid reactive substance assay [21]. The SOD concentration assay was performed strictly according to the SOD assay kit instructions.

2.8. RNA isolation and qRT-PCR

The tissue mRNA transcription levels of the different cytokines were analyzed using qRT-PCR. The ovarian tissue was crushed in liquid nitrogen to extract the total RNA, which was then transcribed to obtain cDNA. The expression of the mRNA of specific genes was subjected to the fluorescence intensity of SYBR Green I during PCR. The primers used are given in Table S1 (Supplementary Materials). Finally, the interest gene levels were normalized based on the level of β-actin mRNA and computed through the $2^{-\Delta\Delta Ct}$ method.

2.9. Proteomic analysis of ovary proteins

After the collected ovarian tissue was ground in a strong radioimmunoprecipitation assay buffer (PMK0213), the protein concentration in the supernatant was determined using a BCA kit. After the proteins from the ovaries were extracted, quantified, and then digested with trypsin into peptides according to previously described methods [39], these peptides were determined using high-resolution liquid chromatography-mass spectrometry/mass spectrometry (LC-MS/MS). The mass spectrum diagrams were analyzed using Proteome Discover 2.0 software, and the background database was downloaded from Uni Prot (https://www.uniprot.org/). The protein data were analyzed through the DAVID Bioinformatics Resources 6.8 website (https://david.ncifcrf.gov/).

2.10. Immunohistochemistry assay of p-Smad3

For the immunohistochemistry assay, ovarian tissue slices were deparaffinized and dehydrated in graded ethanol solutions. Sections were blocked for 2 h with 5% bovine serum albumin in Tris. Subsequently, immunohistochemistry (IHC) analyses were performed following the standard streptavidin-biotin-peroxidase method. Slices were cultured with a primary antibody against *p*-Smad3 (bs-3425R, 1:900, Bioss) at 4 °C overnight, then treated with the secondary antibody coupled with HRP for 30 min at 25 °C. Finally, sections were digitized with a NanoZoomer S360 (Hamamatsu, Japan) slide scanner. Five fields were selected randomly in each section, and Image J software was used to determine the integrated optical density of *p*-Smad3 positive staining in ovarian tissue.

2.11. Statistical analysis

The data and error bars are shown as means ± standard error of the mean. GraphPad Prism 8.0.2 (San Diego, CA, USA) was used to create the graphs. One-way analysis of variance with Tukey's test or Fisher's least-significant difference test was used to distinguish the significant differences. Differences were regarded as significant or extremely significant when $p < 0.05$ or $p < 0.01$, respectively.

3. Results

3.1. Co-exposure increased the number of cystic and atretic follicles

Hematoxylin-eosin staining was used to determine any histopathological changes in the ovaries of rats exposed to MPs and DEHP, alone or combined. The ovarian samples from the saline group exhibit normal follicles at all phases of growth. The corpus luteum and the granulosa cells within the follicles are arranged tightly and regularly with no obvious abnormalities (Fig. 1a). In the groups exposed to MPs and DEHP alone or in combination, follicular structural abnormalities, such as granulosa cell detachment and flocculent oocyte nuclear chromatin, are conspicuous. We observed follicular cysts and abnormal hemorrhaging in the ovarian medulla in samples from the combined exposure group, which were not seen in the saline or separate exposure groups. The numbers of secondary and atretic follicles were slightly higher in the MPs or DEHP-alone treatment groups than in the saline group (Fig. 1b), but these were not statistically significant. However, there was a sharp increase in secondary and atretic follicles when comparing the MPs and DEHP (0.3) mixed treatment groups with the control group.

3.2. Co-exposure aggravates ovarian fibrosis

Ovarian fibrosis is a notable feature of PCOS patients. The Masson's trichrome staining results show the deposition of collagen in the ovaries (Fig. 2a). The blue collagen volume fraction was remarkably higher in the MP ($p < 0.01$), MP + L-DEHP ($p < 0.05$), and MP + H-DEHP ($p < 0.001$) groups than in the saline group (Fig. 2b). Simultaneous exposure to MPs and DEHP led to pronounced collagen deposition. Samples from the MP + H-DEHP group showed the most severe fibrosis among all treatment groups. The results of qRT-PCR (Fig. 2c and d) and ELISA (Fig. 2e and f) indicate that type I and type III collagen are remarkably upregulated in the MP + H-DEHP group compared with the saline group ($p < 0.05$). Compared to exposure to DEHP or MPs alone, co-exposure to DEHP and MPs resulted in a greater expression of *Col1a1* and *Col3a1* (Fig. 2e and f), consistent with the results of ovarian fibrosis.

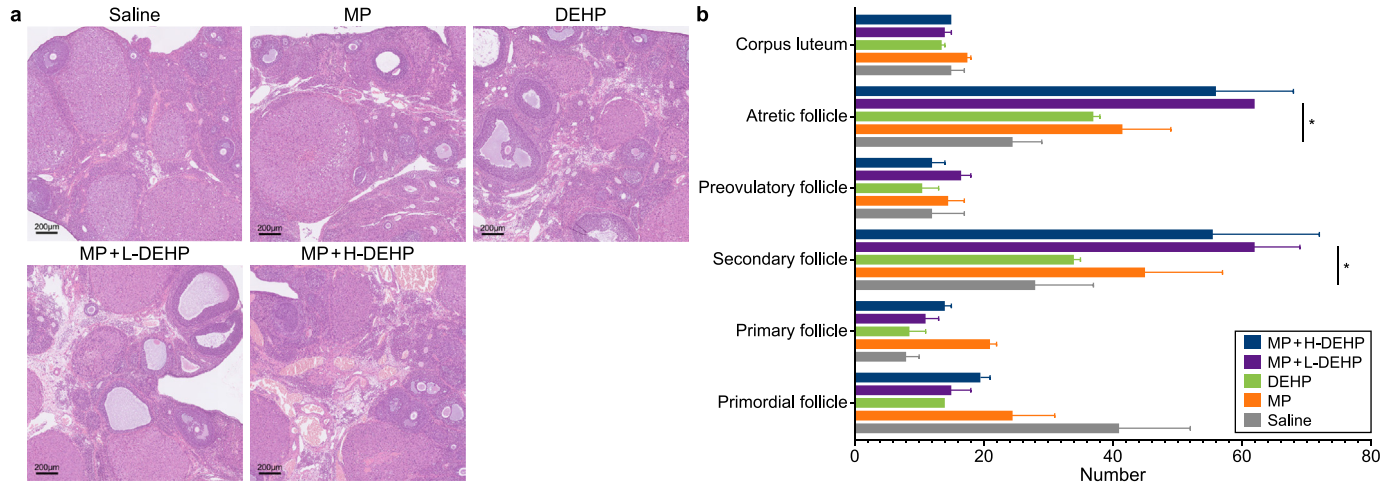

Fig. 1. Pathological lesions in ovarian tissue and follicle counts. **a**, H&E staining of ovaries. **b**, The number of follicles at each stage. *: $p < 0.05$. The asterisks (*) indicate the comparison with the control group.

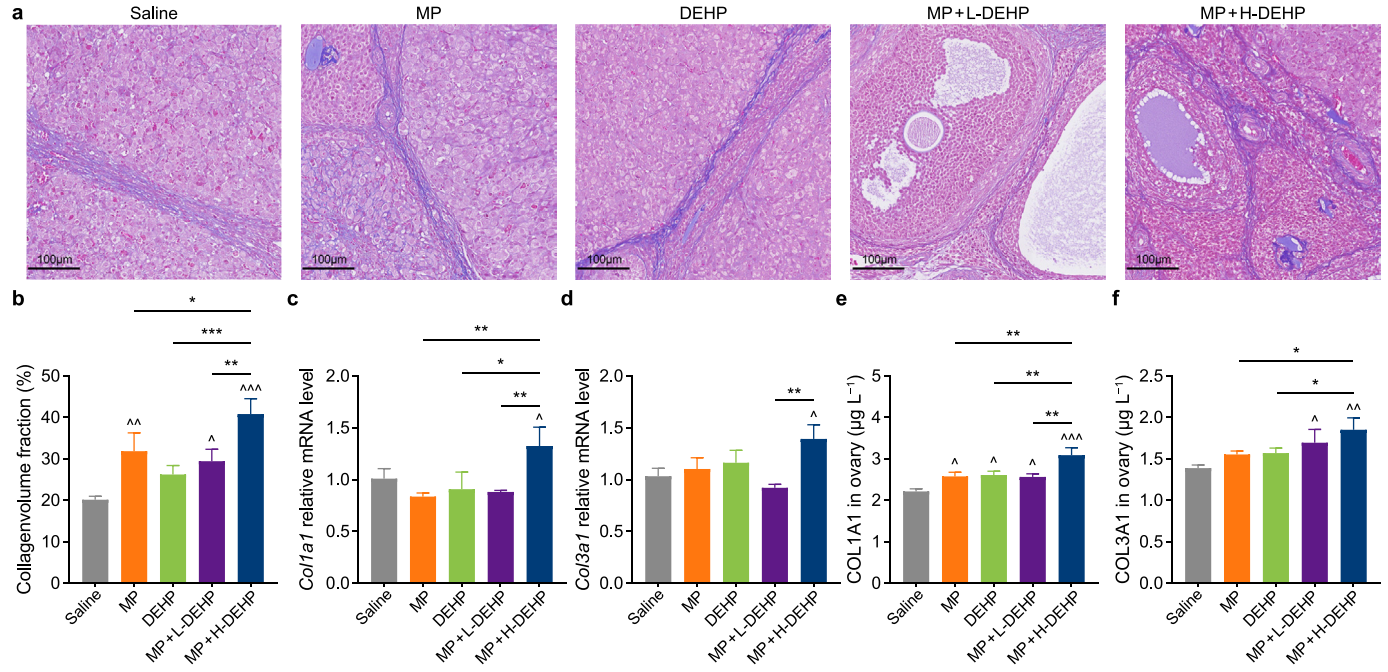

Fig. 2. Fibrosis of ovarian tissue. **a**, Masson-trichrome staining of ovaries. **b**, Collagen volume fraction. **c**, The mRNA level of *Col1a1*. **d**, The mRNA level of *Col3a1*. **e**, ELISA determination of COL1A1 concentration in ovaries. **f**, ELISA determination of COL3A1 concentration in ovaries. * or ^: $p < 0.05$; ** or ^^: $p < 0.01$; *** or ^^^: $p < 0.001$. ^, ^^, or ^^^ on the bar indicates the comparison with the control group; *, **, or *** on the short lines indicate the comparison between the two groups indicated.

3.3. Co-exposure triggers sex hormone disorders in the serum

Concentrations of E2 and T in serum were measured using ELISA kits. Exposure to PS-MPs or DEHP separately induced a small decrease in serum E2 levels, while co-exposure induced a remarkable decrease in E2 levels compared with the control group (Fig. 3a). The data for T content (Fig. 3b) showed a remarkable increase in the MP + L-DEHP samples ($p < 0.01$) and the MP + H-DEHP samples ($p < 0.05$), with the MP + L-DEHP group exhibiting the greatest increase. A remarkable decline in the ratio of E2 to T has been reported in females with PCOS [40,41], and the same tendency has been observed in PCOS model rats in other animal experiments [42]. We plotted bar graphs based on the ratio of E2 to T (Fig. 3c). The E2/T ratio was downregulated in all four dosage groups compared to the saline group, with statistically significant results caused by MP + L-DEHP treatment ($p < 0.05$) and MP + H-DEHP ($p < 0.05$) treatment.

3.4. Proteomic changes in the ovary

To explore the underlying mechanisms of ovarian damage resulting from exposure to one or both MPs and DEHP, we performed a proteomic analysis of ovarian protein. At the end of the 42-day exposure period, a total of 2492 proteins were detected using LC-MS/MS. Their intersection is shown in the Venn diagram (Fig. 4a). Differentially expressed proteins in each group were

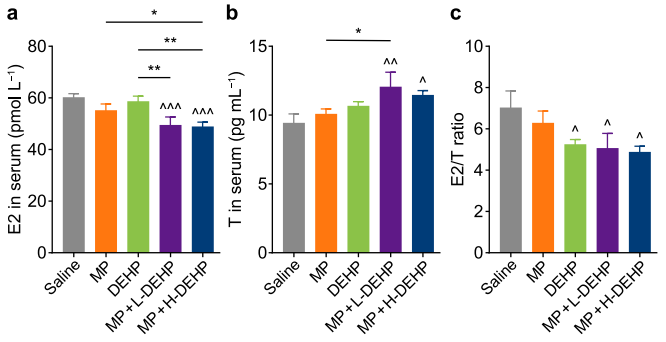

Fig. 3. Dyshomeostasis of sex hormones. a, E2 levels in serum. **b**, T levels in serum. **c**, E2/T ratio. * or ^: $p < 0.05$; ** or ^^: $p < 0.01$; ^^^: $p < 0.001$. ^, ^^, or ^^^ on the bar indicate the comparison with the control group; *, **, or *** on the short lines indicate the comparison between the two groups indicated.

screened using the peak area of the spectra as a proxy for protein abundance (absolute $\log_2$ (fold change) > 1, $p < 0.05$). Compared with the saline group, there were 234 differentially expressed proteins identified in the MP exposure group (80 downregulated proteins, 154 upregulated proteins), 300 in the DEHP group (58 downregulated proteins, 242 upregulated proteins), 199 in the MP + L-DEHP group (68 downregulated proteins, 131 upregulated proteins), and 155 in the MP + H-DEHP group (100 downregulated proteins, 55 upregulated proteins). The volcano plots showing the differentially expressed protein profile of each group are given in Fig. 4b.

We summarized all the differentially expressed proteins based on the volcano plots to identify commonality. There are overlapping areas of differentially expressed proteins caused by exposure to MPs or DEHP alone or together, such as P62260, Q63617, and P41542. These shared differentially expressed proteins suggest that MPs and DEHP alone or together may have synergistic effects on the above pathways.

Kyoto encyclopedia of genes and genomes (KEGG) enrichment analysis of the differentially expressed proteins was performed (Fig. 5). There were 12 common pathways in the enrichment results of the combined exposure groups, such as oxidative phosphorylation [2] and chemical carcinogenesis – reactive oxygen species [43], which have been confirmed in previous studies. Notably, the enrichment analysis of all treatment groups identified five pathways: the metabolic pathway, nucleotide metabolism, fatty acid metabolism, tight junction, and prion disease. The differentially expressed proteins identified in these five pathways are detailed in Table S2 (Supplementary Materials). This suggests that MPs and DEHP, administered alone or to rats, may have synergistic effects in these pathways. Patients with PCOS are often characterized by obesity and ovarian fibrosis. Of the aforementioned pathways, fatty acid metabolism and tight junctions are closely related to these characteristics. Furthermore, both the fatty acid metabolism and tight junction pathways are regulated by TGF-β1 [44,45]. Therefore, we employed SIS3 to selectively inhibit *p*-Smad3 generation in subsequent experiments.

3.5. Co-exposure activates the TGF-β1/Smad3 signaling pathway

Ovarian fibrosis is common in patients with PCOS, and the TGF-β1/Smad3 signaling pathway has a vital role in the fibrosis of various organs. To investigate whether exposure to MPs, DEHP, or a combination of the two can induce changes in the above signaling pathway, we detected the gene activity of TGF-β1 and Smad3 through qRT-PCR, and the tissue content of TGF-β1 and Smad3 through ELISA.

The ELISA results showed that the concentration of TGF-β1 in ovarian tissue was significantly high after co-exposure, but it returned to normal levels after SIS3 treatment (Fig. 6c). There was a similar trend in TGF-β1 at the mRNA levels (Fig. 6e). The Smad3 mRNA levels (Fig. 6d) were conspicuously upregulated in the MP

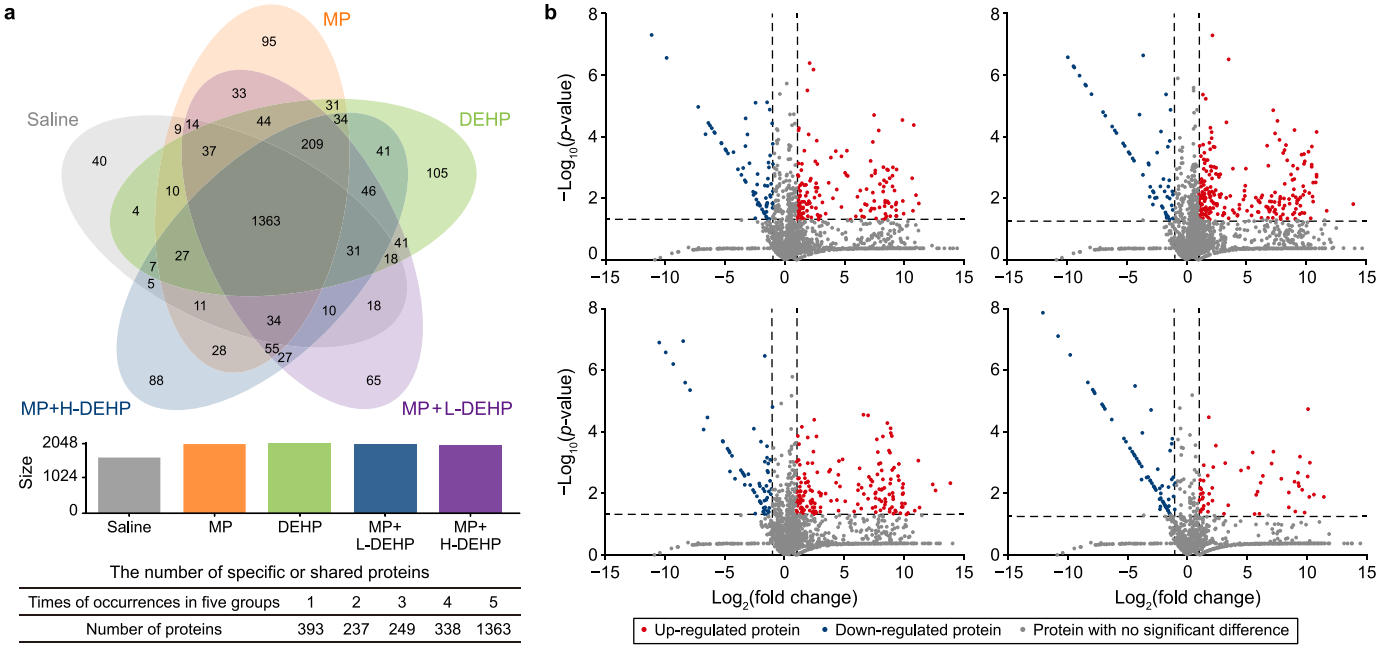

Times of occurrences in five groups	1	2	3	4	5
Number of proteins	393	237	249	338	1363

Fig. 4. Identification of differentially expressed proteins. a, The Venn diagram of co-expressed proteins in the ovarian. The columns indicate the number of proteins in each group. The bottom table shows the number of specific or shared proteins. **b**, The volcano plots (from top to bottom and left to right): Saline group vs. MP group, Saline group vs. DEHP group, Saline group vs. MP + L-DEHP group, Saline group vs. MP + H-DEHP group. Red points: up-regulated protein, fold change >2 and $p < 0.05$; Blue points: down-regulated protein, fold change <0.5 and $p < 0.05$; Gray points: protein with non-significantly different proteins, absolute $\log_2$ (fold change) < 1 or $p > 0.05$.

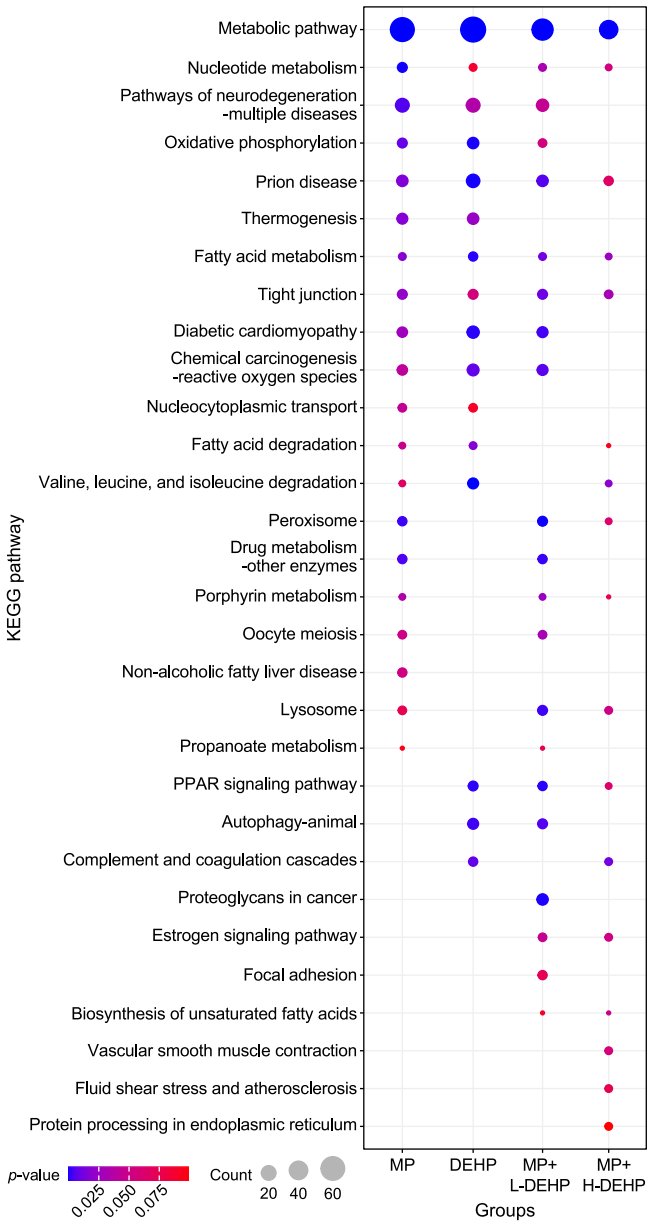

Fig. 5. KEGG enrichment of differentially expressed proteins.

group, DEHP group, and co-exposure group compared with the saline group. Fig. 6a depicts representative images of the anti-*p*-Smad3 immunohistochemistry results. As shown in the statistical results (Fig. 6b), the density of *p*-Smad3 positive staining was conspicuously higher in the MP, DEHP, and MP + H-DEHP groups than in the saline group. Treatment with SIS3 inhibited the production of *p*-Smad3, particularly in the MP + H-DEHP group. It should be noted that *p*-Smad3 increased more significantly in the MP + H-DEHP group samples than in the MP and MP + L-DEHP groups. In addition, Smad3 mRNA levels were also upregulated, with the most significant increase being in the MP + H-DEHP group.

3.6. Co-exposure increases levels of oxidative stress markers

The MP + H-DEHP treatment resulted in highly significant increases in ROS and MDA levels and SOD activity in the ovarian tissues compared with the saline group (Supplementary Material Fig. S3). The MP + H-DEHP group had conspicuously higher ROS and MDA levels and SOD activity than the other MP and DEHP groups. The levels of all three markers were significantly lower in the MP + H-DEHP + SIS3 group than in the MP + H-DEHP group.

3.7. Blocking TGF-β1/Smad3 alleviated PCOS symptoms

The impact of SIS3 treatment was evaluated in terms of fibrosis and sex hormone homeostasis. The effect of the inhibitor SIS3 can be seen in ovarian fibrosis. The collagen volume fraction was reduced significantly in the MP + SIS3 group compared with the MP group ($p < 0.001$). Similarly, the collagen volume fraction dropped significantly in the MP + H-DEHP + SIS3 group compared with the MP + H-DEHP group ($p < 0.05$). The other Masson's trichrome-stained sections of the ovaries are shown in Fig. 7a. At the mRNA level (Fig. 7d and e), and the protein level (Fig. 7b and c), the upregulation of *Col1a1* and *Col3a1* was mitigated by the effect of SIS3. A comparison of the MP + H-DEHP and MP + H-DEHP + SIS3 groups shows that SIS3 treatment increased E2 levels and decreased T levels (Fig. 7g–i).

4. Discussion

Although the toxicity of MPs and their co-exposure with plasticizers has been extensively explored in recent years, the complex toxicity mechanisms of concurrent MPs and DEHP exposure are not fully understood. Recently, one study showed that exposure to 100 mg PS-MPs L^{-1} and 200 mg DEHP kg^{-1} for 35 days destroys the ovarian granulosa cell layer in mice, leading to follicular fragmentation and atresia. By contrast, low doses and long exposures are environmentally relevant. In this work, we examined the response to MPs and DEHP exposure at the proteomic level, which was not previously reported. Our findings indicated that the adverse effects resulting from simultaneous exposure to MPs and DEHP on the ovaries are highly consistent with PCOS symptoms, such as the increased number of cystic and atretic follicles, raised serum T levels, decreased E2 levels, high oxidative stress levels, ovarian fibrosis, and increased expression of TGF-β1 and *p*-Smad3. We also showed that SIS3 treatment restrains *p*-Smad3 and significantly alleviates the adverse effects, suggesting that the TGF-β1/Smad3 signaling pathway plays a major role in the toxicological mechanism underlying the negative impact of combined exposure to MPs and DEHP.

The Rotterdam criteria (2003) are the most universally accepted criteria for diagnosing PCOS, an ovarian dysfunction condition whose main features are hyperandrogenism and polycystic ovary morphology [46]. The appearance of these features received special attention in this study (Fig. 1). An et al. showed that ingesting PS-MPs for 90 consecutive days increases oxidative stress levels in rat ovaries and activates the Wnt/β-Catenin pathway causing fibrosis in ovaries [20]. This is consistent with the results of our study. Polycystic ovary syndrome also exhibits the features of enhanced TGF-β1 activity, with enhanced fibrous tissue and collagen in the ovarian envelope or the ovarian medulla and interstitium (Fig. 2). We showed that simultaneous exposure to MPs and DEHP can aggravate the above symptoms.

Exposure to MPs and DEHP in combination or alone can cause significantly elevated levels of oxidative stress in ovarian tissue. Oxidative stress affects an extensive range of physiological and pathological functions in the ovary and is widespread in patients with PCOS [47]. Oocyte maturation, folliculogenesis, ovarian steroidogenesis, and luteolysis may be modulated by ROS [48]. Reactive oxygen species is one of the factors influencing the formation of cystic follicles and the number of atretic follicles, and it affects

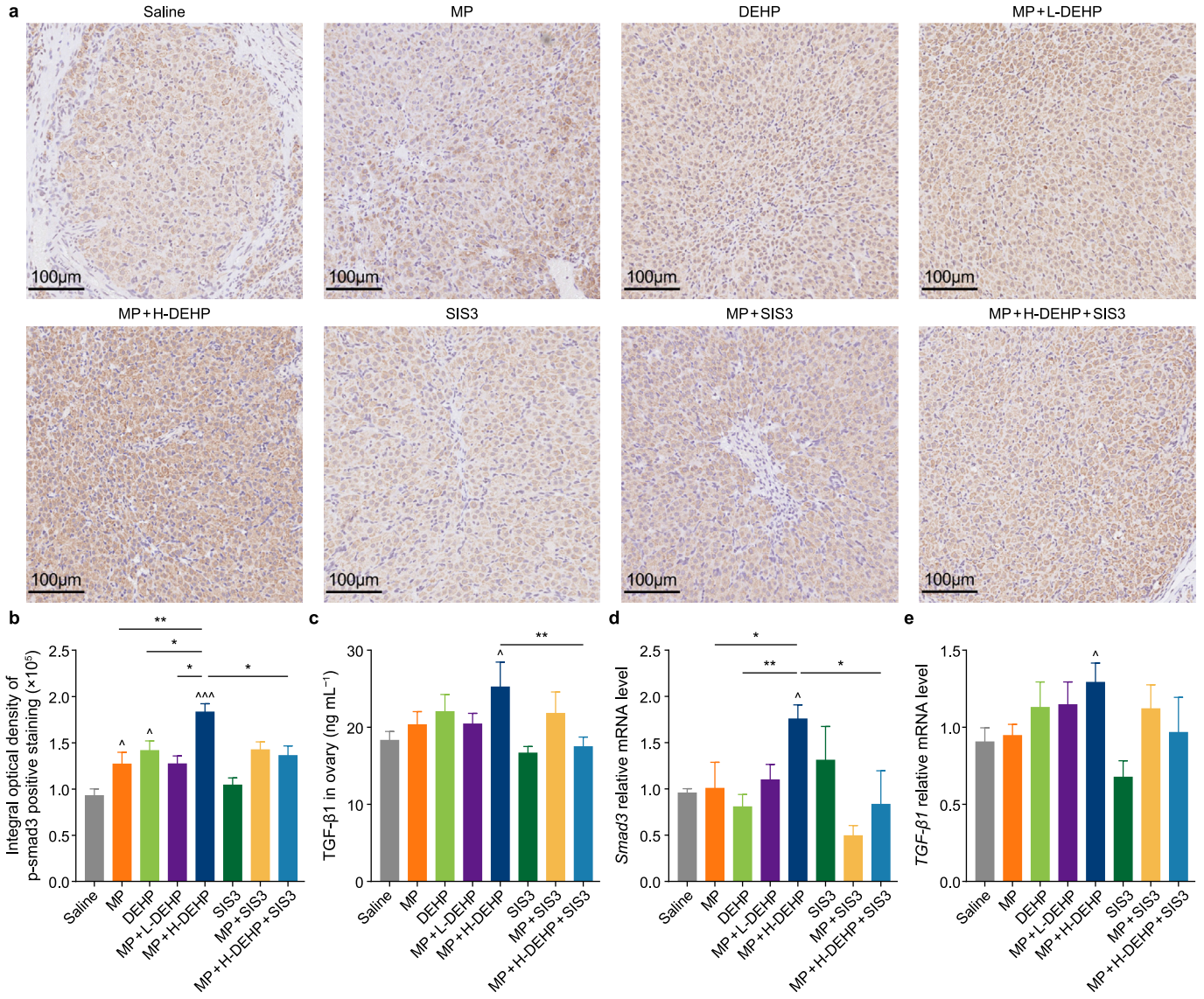

Fig. 6. Co-exposure activates the TGF-β1/Smad3 signaling pathway. a, Immunohistochemistry for *p*-Smad3. **b**, The integral optical density of *p*-Smad3. **c**, TGF-β1 concentration in ovaries. **d**, The mRNA levels of *p*-Smad3 in ovaries. **e**, The mRNA levels of TGF-β1 in ovaries. * or ^: $p < 0.05$; **: $p < 0.01$; ***: $p < 0.001$. ^ or ^^^ on the bar indicate the comparison with the control group; * or ** on the short lines indicate the comparison between the two groups indicated.

hormonal balance. Granulosa cells can regulate follicular development by converting T to E2. Reactive oxygen species-induced granulosa cell apoptosis may explain the decrease in estradiol levels [49]. In this research, we found that although the changes in hormone levels and the number of cystic and atretic follicles formed are insignificant, the injury is more severe in the combined exposure group. This may be due to simultaneous exposure to MPs and DEHP, which causes more severe oxidative stress than MPs or DEHP alone, an explanation supported by previous studies [43].

Fibrosis of the ovaries is one of the principal reproductive disorders in women. We showed in this work that the expression of type I and type III collagen is remarkably upregulated, and increased collagen deposition in the ovaries of the rats exposed to both PS-MPs and DEHP is observed. TGF-β1 regulates collagen expression in tissues, and SIS3 mitigates fibrosis (Fig. 6). There is a crosstalk between oxidative stress and the TGF-β1/Smad3 pathway [50,51]. In this work, the experimental results indicated that retarding the TGF-β1/Smad3 pathway also reduces the levels of oxidative stress markers. Tissue damage induced by PS-MPs and DEHP may generate more ROS, which is a vicious cycle; however, SIS3 can break this cycle, alleviating oxidative stress. Overexpression of TGF-β1 also inhibits the conversion of testosterone to estradiol [31], which may cause hormonal imbalance. Therefore, it is noteworthy that the MP + H-DEHP group exhibits the strongest TGF-β1and *p*-Smad3 activity among all groups, suggesting that the TGF-β1/Smad3 pathway may be a common pathway for both toxins to exert their effects.

Kyoto encyclopedia of genes and genomes enrichment reveals potential synergistic impacts from exposure to MPs and DEHP on the metabolic pathway, nucleotide metabolism, fatty acid metabolism, tight junctions, and prion disease. This implies that co-exposure may contribute to metabolic abnormalities and biological barrier breakthroughs in mammals. As the first three impacts presented above belong to the category of metabolic impairment and the fact that obesity is common among PCOS patients, fatty acid metabolism and tight junctions have received special attention. The

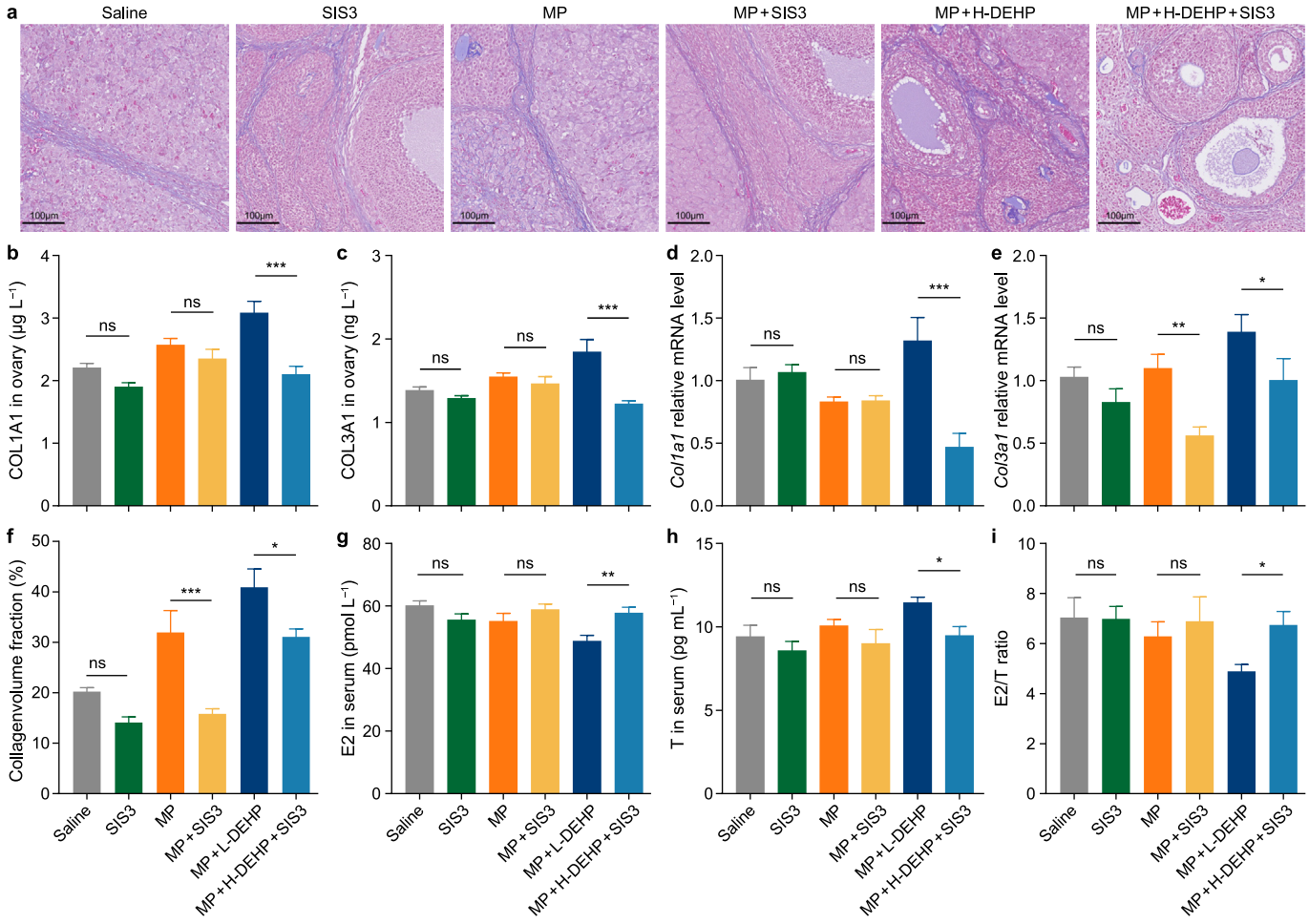

Fig. 7. SIS3 alleviated ovarian fibrosis and sex hormone disorders. **a**, Masson-trichrome staining of ovaries. **b**, ELISA determination of COL1A1 concentration in ovaries. **c**, ELISA determination of COL3A1 concentration in ovaries. **d**, The mRNA levels of *Col1a1*. **e**, The mRNA levels of *Col3a1*. **f**, Collagen volume fraction. **g**, E2 concentration in serum. **h**, T concentration in serum. **i**, E2/T ratio. Panels **g**–**i** show the restoration of sex hormone homeostasis with SIS3 treatment. *: $p < 0.05$; **: $p < 0.01$; ***: $p < 0.001$; ns: no signification. *, **, or *** on the short lines indicate the comparison between the two groups indicated.

hypothesis that MPs cause metabolic abnormalities in rodents has been demonstrated in previous studies. Wang et al. showed that oral administration of 30 mg PS-NPs kg^{-1} day^{-1} remarkably increases fasting glucose levels, glucose intolerance, and insulin resistance in mice [52]. In our results, the upregulation of proteins, such as Q5PPL3, Q62904, Q64654, and Q5XI22, in the combined treatment group compared with the saline group indicated that increased lipid synthesis in rats is due to the combined effect of DEHP and MPs. Serum lipid content verifies the increase in lipid synthesis (Supplementary Material Fig. S4). Microplastics and DEHP are also thought to increase the risk of intercellular tight junction damage. Dissolution of intercellular adhesion molecules is a common form of tight junction injury. A0A0G2K2P5, Q66HL2, and Q9JLT0, which are all involved in intercellular adhesion, are remarkably downregulated in all treatment groups compared to the saline control group. In addition, the dissolution of intercellular adhesion molecules is an early reaction of extracellular matrix deposition [53], and TGF-β1/Smad3 is a common factor affecting extracellular matrix deposition. Zhang et al. showed that in HK-2 cells, the mRNA activity and protein content of ZO-1 and occludin decrease time-dependent after TGF-β1 treatment [54]. The abnormal tight junctions identified in the enrichment results of this study may be a consequence of the activation of TGF-β1/Smad3 signaling.

5. Conclusion

This study demonstrated that co-exposure to DEHP and MPs induced reproductive toxicity in female rats, resulting in PCOS-like ovarian features, such as an increased number of cystic follicles, dysregulation of sex hormone homeostasis, oxidative stress, and fibrosis. Reducing TGF-β1/Smad3 activity can lessen the production of ROS and alleviate the imbalance of sex hormone homeostasis and the degree of ovarian fibrosis. Our study was the first to investigate the synergistic mechanism of co-exposure to DEHP and MPs at the proteomic level, showing synergistic effects on metabolic abnormalities and tight junction damage. This provides a reference for the correlation of simultaneous exposure to DEHP and MPs and female reproductive disorders.

CRediT authorship contribution statement

Ke Xu: Writing - Original Draft, Methodology, Investigation, Data Curation, Validation. **Yunyi Wang:** Methodology. **Xiao Gao:** Methodology, Software. **Zhaolan Wei:** Investigation. **Qi Han:** Investigation. **Shuxin Wang:** Methodology. **Wanting Du:** Methodology. **Jian Wan:** Methodology. **Cuihong Wan:** Methodology. **Mingqing Chen:** Writing - Review & Editing, Supervision, Project Administration, Methodology, Funding Acquisition, Conceptualization.

Declaration of competing interest

The authors declare that they have no known competing financial interests or personal relationships that could have appeared to influence the work reported in this paper.

Acknowledgments

The National Natural Science Foundation of China (42277437) sponsored this research. We are grateful to Dr. Zheng Zhang from CCNU for help with the proteomic analysis. We want to thank Prof. Zhihong Zhu from CCNU for identifying PS-MPs.

Appendix A. Supplementary data

Supplementary data to this article can be found online at https://doi.org/10.1016/j.ese.2024.100471.

References

[1] UNEP, UNEP, Valuing Plastics: the Business Case for Measuring, Managing and Disclosing Plastic Use in the Consumer Goods Industry, 2014, 2014.
[2] Z. Liu, Q. Zhuan, L. Zhang, L. Meng, X. Fu, Y. Hou, Polystyrene microplastics induced female reproductive toxicity in mice, J. Hazard Mater. 424 (Pt C) (2022) 127629.
[3] B. Jiang, A.E. Kauffman, L. Li, W. McFee, B. Cai, J. Weinstein, J.R. Lead, S. Chatterjee, G.I. Scott, S. Xiao, Health impacts of environmental contamination of micro- and nanoplastics: a review, Environ. Health Prev. Med. 25 (1) (2020) 29.
[4] E. Danopoulos, M. Twiddy, J.M. Rotchell, Microplastic contamination of drinking water: a systematic review, PLoS One 15 (7) (2020) e0236838.
[5] W. Nicole, Microplastics in seafood: how much are people eating? Environ. Health Perspect. 129 (3) (2021) 34001.
[6] P. Farrell, K. Nelson, Trophic level transfer of microplastic: Mytilus edulis (L.) to Carcinus maenas (L.), Environ. Pollut. 177 (2013) 1–3.
[7] A.D. Vethaak, J. Legler, Microplastics and human health, Science 371 (6530) (2021) 672–674.
[8] K. Senathirajah, S. Attwood, G. Bhagwat, M. Carbery, S. Wilson, T. Palanisami, Estimation of the mass of microplastics ingested - a pivotal first step towards human health risk assessment, J. Hazard Mater. 404 (Pt B) (2021) 124004.
[9] J. Xu, W. Bi, L. Hua, Z. Cheng, Y. Wang, D. Li, W. Liu, L. Wang, H. Sun, Wide occurrence of seven phthalate plasticizers and two typical microplastics in pig feed, Chemosphere 307 (Pt 2) (2022) 135847.
[10] B. Rios-Fuster, C. Alomar, G. Paniagua Gonzalez, R.M. Garcinuno Martinez, D.L. Soliz Rojas, P. Fernandez Hernando, S. Deudero, Assessing microplastic ingestion and occurrence of bisphenols and phthalates in bivalves, fish and holothurians from a Mediterranean marine protected area, Environ. Res. 214 (Pt 3) (2022) 114034.
[11] J.N. Hahladakis, C.A. Velis, R. Weber, E. Iacovidou, P. Purnell, An overview of chemical additives present in plastics: migration, release, fate and environmental impact during their use, disposal and recycling, J. Hazard Mater. 344 (2018) 179–199.
[12] H.C. Erythropel, M. Maric, J.A. Nicell, R.L. Leask, V. Yargeau, Leaching of the plasticizer di(2-ethylhexyl)phthalate (DEHP) from plastic containers and the question of human exposure, Appl. Microbiol. Biotechnol. 98 (24) (2014) 9967–9981.
[13] Y. Deng, Z. Yan, R. Shen, M. Wang, Y. Huang, H. Ren, Y. Zhang, B. Lemos, Microplastics release phthalate esters and cause aggravated adverse effects in the mouse gut, Environ. Int. 143 (2020) 105916.
[14] S. Wang, Q. Han, Z. Wei, Y. Wang, J. Xie, M. Chen, Polystyrene microplastics affect learning and memory in mice by inducing oxidative stress and decreasing the level of acetylcholine, Food Chem. Toxicol. 162 (2022) 112904.
[15] X. Xie, T. Deng, J. Duan, J. Xie, J. Yuan, M. Chen, Exposure to polystyrene microplastics causes reproductive toxicity through oxidative stress and activation of the p38 MAPK signaling pathway, Ecotoxicol. Environ. Saf. 190 (2020) 110133.
[16] H. Jin, T. Ma, X. Sha, Z. Liu, Y. Zhou, X. Meng, Y. Chen, X. Han, J. Ding, Polystyrene microplastics induced male reproductive toxicity in mice, J. Hazard Mater. 401 (2021) 123430.
[17] S. Wen, Y. Chen, Y. Tang, Y. Zhao, S. Liu, T. You, H. Xu, Male reproductive toxicity of polystyrene microplastics: study on the endoplasmic reticulum stress signaling pathway, Food Chem. Toxicol. 172 (2023) 113577.
[18] Y. Deng, Z. Yan, R. Shen, Y. Huang, H. Ren, Y. Zhang, Enhanced reproductive toxicities induced by phthalates contaminated microplastics in male mice (Mus musculus), J. Hazard Mater. 406 (2021) 124644.
[19] D. Li, W. Sun, X. Jiang, Z. Yu, Y. Xia, S. Cheng, L. Mao, S. Luo, S. Tang, S. Xu, Z. Zou, C. Chen, J. Qiu, L. Zhou, Polystyrene nanoparticles enhance the adverse effects of di-(2-ethylhexyl) phthalate on male reproductive system in mice, Ecotoxicol. Environ. Saf. 245 (2022) 114104.
[20] R. An, X. Wang, L. Yang, J. Zhang, N. Wang, F. Xu, Y. Hou, H. Zhang, L. Zhang, Polystyrene microplastics cause granulosa cells apoptosis and fibrosis in ovary through oxidative stress in rats, Toxicology 449 (2021) 152665.
[21] Z. Wei, Y. Wang, S. Wang, J. Xie, Q. Han, M. Chen, Comparing the effects of polystyrene microplastics exposure on reproduction and fertility in male and female mice, Toxicology 465 (2022) 153059.
[22] B. Trnka, M. Polan, V.A. Zigmont, Exposure to Di-2-ethylhexyl phthalate (DEHP) and infertility in women, NHANES 2013-2016, Reprod. Toxicol. 103 (2021) 46–50.
[23] W. Zhan, H. Yang, J. Zhang, Q. Chen, Association between co-exposure to phenols and phthalates mixture and infertility risk in women, Environ. Res. 215 (Pt 1) (2022) 114244.
[24] C.S. da Costa, T.F. Oliveira, L.C. Freitas-Lima, A.S. Padilha, M. Krause, M. Carneiro, B.S. Salgado, J.B. Graceli, Subacute cadmium exposure disrupts the hypothalamic-pituitary-gonadal axis, leading to polycystic ovarian syndrome and premature ovarian failure features in female rats, Environ. Pollut. 269 (2021) 116154.
[25] N.F. Goodman, R.H. Cobin, W. Futterweit, J.S. Glueck, R.S. Legro, E. Carmina, E. American Association of Clinical, E. American College of, E. Androgen, P. Society, American association of clinical endocrinologists, American college of endocrinology, and androgen excess and pcos society disease state clinical review: guide to the best practices in the evaluation and treatment of polycystic ovary syndrome - Part 2, Endocr. Pract. 21 (12) (2015) 1415–1426.
[26] I. Ortega, A.B. Cress, D.H. Wong, J.A. Villanueva, A. Sokalska, B.C. Moeller, S.D. Stanley, A.J. Duleba, Simvastatin reduces steroidogenesis by inhibiting Cyp17a1 gene expression in rat ovarian theca-interstitial cells, Biol. Reprod. 86 (1) (2012) 1–9.
[27] Y. Zhou, H. Lan, Z. Dong, W. Li, B. Qian, Z. Zeng, W. He, J.L. Song, Rhamnocitrin attenuates ovarian fibrosis in rats with letrozole-induced experimental polycystic ovary syndrome, Oxid. Med. Cell. Longev. 2022 (2022) 5558599.
[28] R. Tal, D.B. Seifer, A. Shohat-Tal, R.V. Grazi, H.E. Malter, Transforming growth factor-beta1 and its receptor soluble endoglin are altered in polycystic ovary syndrome during controlled ovarian stimulation, Fertil. Steril. 100 (2) (2013) 538–543.
[29] K.J. Gordon, G.C. Blobe, Role of transforming growth factor-beta superfamily signaling pathways in human disease, Biochim. Biophys. Acta 1782 (4) (2008) 197–228.
[30] L. Cui, H. Bao, Z. Liu, X. Man, H. Liu, Y. Hou, Q. Luo, S. Wang, Q. Fu, H. Zhang, hUMSCs regulate the differentiation of ovarian stromal cells via TGF-beta(1)/Smad3 signaling pathway to inhibit ovarian fibrosis to repair ovarian function in POI rats, Stem Cell Res. Ther. 11 (1) (2020) 386.
[31] X. Zheng, C.A. Price, Y. Tremblay, J.G. Lussier, P.D. Carriere, Role of transforming growth factor-beta1 in gene expression and activity of estradiol and progesterone-generating enzymes in FSH-stimulated bovine granulosa cells, Reproduction 136 (4) (2008) 447–457.
[32] C. Kilkenny, W.J. Browne, I.C. Cuthill, M. Emerson, D.G. Altman, Improving bioscience research reporting: the ARRIVE guidelines for reporting animal research, Osteoarthritis Cartilage 20 (4) (2012) 256–260.
[33] H. Wu, D. Wang, H. Shi, N. Liu, C. Wang, J. Tian, X. Wang, Z. Zhang, PM(2.5) and water-soluble components induce airway fibrosis through TGF-beta1/Smad3 signaling pathway in asthmatic rats, Mol. Immunol. 137 (2021) 1–10.
[34] J.L. Lyche, A.C. Gutleb, A. Bergman, G.S. Eriksen, A.J. Murk, E. Ropstad, M. Saunders, J.U. Skaare, Reproductive and developmental toxicity of phthalates, J. Toxicol. Environ. Health B Crit. Rev. 12 (4) (2009) 225–249.
[35] S. Wang, Q. Han, Z. Wei, Y. Wang, L. Deng, M. Chen, Formaldehyde causes an increase in blood pressure by activating ACE/AT1R axis, Toxicology 486 (2023) 153442.
[36] A.L. Winship, U.C. Sarma, L.R. Alesi, K.J. Hutt, Accurate follicle enumeration in adult mouse ovaries, J. Vis. Exp. 164 (2020).
[37] M. Myers, K.L. Britt, N.G. Wreford, F.J. Ebling, J.B. Kerr, Methods for quantifying follicular numbers within the mouse ovary, Reproduction 127 (5) (2004) 569–580.
[38] C. Du, J. Kang, W. Yu, M. Chen, B. Li, H. Liu, H. Wang, Repeated exposure to temperature variation exacerbates airway inflammation through TRPA1 in a mouse model of asthma, Respirology 24 (3) (2019) 238–245.
[39] N. Pan, Z. Wang, B. Wang, J. Wan, C. Wan, Mapping microproteins and ncRNA-encoded polypeptides in different mouse tissues, Front. Cell Dev. Biol. 9 (2021) 687748.
[40] J. Chen, S. Shen, Y. Tan, D. Xia, Y. Xia, Y. Cao, W. Wang, X. Wu, H. Wang, L. Yi, Q. Gao, Y. Wang, The correlation of aromatase activity and obesity in women with or without polycystic ovary syndrome, J. Ovarian Res. 8 (2015) 11.
[41] A. Li, L. Zhang, J. Jiang, N. Yang, Y. Liu, L. Cai, Y. Cui, F. Diao, X. Han, J. Liu, Y. Sun, Follicular hyperandrogenism and insulin resistance in polycystic ovary syndrome patients with normal circulating testosterone levels, J Biomed Res 32 (3) (2017) 208–214.
[42] S. Song, Y. Tan, Expression of FKBP52 in the ovaries of PCOS rats, Int. J. Mol. Med. 43 (2) (2019) 868–878.
[43] H. Wu, Q. Liu, N. Yang, S. Xu, Polystyrene-microplastics and DEHP co-exposure induced DNA damage, cell cycle arrest and necroptosis of ovarian granulosa cells in mice by promoting ROS production, Sci. Total Environ. 871 (2023) 161962.
[44] C. Caer, C. Rouault, T. Le Roy, C. Poitou, J. Aron-Wisnewsky, A. Torcivia, J.C. Bichet, K. Clement, M. Guerre-Millo, S. Andre, Immune cell-derived cytokines contribute to obesity-related inflammation, fibrogenesis and metabolic deregulation in human adipose tissue, Sci. Rep. 7 (1) (2017) 3000.

[45] L. Zhang, T. Feng, L.J. Spicer, The role of tight junction proteins in ovarian follicular development and ovarian cancer, Reproduction 155 (4) (2018) R183–R198.
[46] Rotterdam ESHRE/ASRM-Sponsored PCOS consensus workshop group, Revised 2003 consensus on diagnostic criteria and long-term health risks related to polycystic ovary syndrome (PCOS), Hum Reprod. 19 (1) (2024) 41–47.
[47] N. Hilali, M. Vural, H. Camuzcuoglu, A. Camuzcuoglu, N. Aksoy, Increased prolidase activity and oxidative stress in PCOS, Clin. Endocrinol. 79 (1) (2013) 105–110.
[48] A. Agarwal, S. Gupta, R.K. Sharma, Role of oxidative stress in female reproduction, Reprod. Biol. Endocrinol. 3 (2005) 28.
[49] A. Tripathi, T.G. Shrivastav, S.K. Chaube, An increase of granulosa cell apoptosis mediates aqueous neem (Azadirachta indica) leaf extract-induced oocyte apoptosis in rat, Int J Appl Basic Med Res 3 (1) (2013) 27–36.
[50] W. Zhu, R.D. Wu, Y.G. Lv, Y.M. Liu, H. Huang, J.Q. Xu, BRD4 blockage alleviates pathological cardiac hypertrophy through the suppression of fibrosis and inflammation via reducing ROS generation, Biomed. Pharmacother. 121 (2020) 109368.
[51] X. Ye, C. Yin, X. Huang, Y. Huang, L. Ding, M. Jin, Z. Wang, J. Wei, X. Li, ROS/TGF-beta signal mediated accumulation of SOX4 in OA-FLS promotes cell senescence, Exp. Gerontol. 156 (2021) 111616.
[52] Y. Wang, Z. Wei, K. Xu, X. Wang, X. Gao, Q. Han, S. Wang, M. Chen, The effect and a mechanistic evaluation of polystyrene nanoplastics on a mouse model of type 2 diabetes, Food Chem. Toxicol. 173 (2023) 113642.
[53] B. Ozdamar, R. Bose, M. Barrios-Rodiles, H.R. Wang, Y. Zhang, J.L. Wrana, Regulation of the polarity protein Par6 by TGFbeta receptors controls epithelial cell plasticity, Science 307 (5715) (2005) 1603–1609.
[54] K. Zhang, H. Zhang, H. Xiang, J. Liu, Y. Liu, X. Zhang, J. Wang, Y. Tang, TGF-beta1 induces the dissolution of tight junctions in human renal proximal tubular cells: role of the RhoA/ROCK signaling pathway, Int. J. Mol. Med. 32 (2) (2013) 464–468.